An Optimized Registration Workflow and Standard Geometric Space for Small Animal Brain Imaging

Horea-Ioan Ioanas[1] Markus Marks[2] Mehmet Fatih Yanik[2] Markus Rudin[1]
[1]Institute for Biomedical Engineering, ETH and University of Zurich
[2]Institute of Neuroinformatics, ETH and University of Zurich

Abstract — As part of the analysis of high-field mouse MRI data, relevant brain tissue needs to be selected via a mask. For this process to be performed automatically, brain voxels need to be classified based both on their signal intensity and position in the image. Nowadays, deep neural networks are the state-of-the-art methods for tissue segmentation in biomedical imaging, and thus constitute a promising method for preclinical neuroscience. We present a deep learning enabled framework for segmentation of brain tissue in functional and structural MR images, *that outperforms* ***current methods****, requiring only a fraction of the processing time needed by them*. **To do** (??)

Background

In order to make meaningful comparisons across subjects inside a study, it is imperative that the images lie in a standard reference frame. Because of positioning imprecision and anatomical animal variations, this is not the case for the original MR acquired images. To solve this issue, the images need to be projected into the reference frame via registration [? ?]. Intensities outside the brain region of a mouse MR image present high variations and bias the registration process. As a remedy, it would be useful to extract the region of interest and perform the registration on it. For this purpose, we propose a machine learning enabled brain extraction in an additional node to the workflow presented by Ioanas et al. [?]. The additional node creates a mask of the brain region with segmentation using a classifier and masks the image such that only the region of interest remains. **To do** (??)

Convolutional Neural Networks

In recent years it has been shown that convolutional neural network give the best results for semantic image segmentation in terms of precision and flexibility [?] [?]. Training a convolutional neural network into a classifier is a supervised method, meaning that the model needs to learn its parameters based on observations of data.

The training data set of a classifier is as important as the architecture of the model itself. To improve general-purpose application, training examples need to be drawn from a usually unknown probability distribution, that is expected to be representative of the space of occurrences. We define the space of occurrences as the space of which the data of interest is drawn from. In our case this consists of all the different mouse brain MRI data sets coming from multiple experiments, with their corresponding labels. Ideally experiment setups are uniform and the resulting data does not differ much, but small variations in the experiment setup and animal size are unavoidable. Based on an approximation of the occurrence space, the network has to build a general model that enables it to extrapolate and produce sufficiently accurate predictions in new cases. Manually creating annotations as required to train a deep-learning classifier for high-resolution data is often infeasible, as it requires manual expert segmentation of vast amounts of slices.

While our purpose was to create a workflow that generates better masks than the ones used for registration**To do** (??), we showed that the latter could be used as training data for the deep-learning model, by applying small changes to them.

The Classifier

Model

As the architecture of the classifier, the U-Net from Ronneberger et al [?] was chosen based on its high performance in the field of biomedical image segmentation. This is a convolutional neural network that consists of a contracting path that captures context in addition to a symmetric expanding path that enables precise localisation. Localisation in this context means that a class label is assigned to each pixel. We used the U-Net implementation from zhixuhao [?], written in Keras. Keras is a high-level neural networks API, written in Python and capable of running on top of TensorFlow, CNTK, or Theano. It allows for a easily readable code and makes it thus easier to reproduce.

The implementation of the U-Net from zhixuhao has two drop-out layers in addition to the original one. A drop-out layer randomly sets a fraction of input units from the layer to 0 at each update during training time. The set fraction rate is 0.5. It is known that dropout helps prevent overfitting and greatly improves the performance of deep learning models [**?**].

Three losses were tested for the training of the model, namely the Dice-loss, the binary-cross-entropy loss and the sum of both.

The Dice-loss is computed from the Dice score. It calculates the similarity of two binary samples X and Y with

$$D_{coef} = \frac{2|X \cap Y|}{|X| + |Y|}$$

It is a quantity ranging from 0 to 1 that is to be maximised. The loss is then calculated with $1-D_{coef}$. Because the Dice loss is not differentiable, small changes need to be made. In our case, the two samples to be compared are normalised, grey valued images and are thus not binary but have values between 0 and 1. Additionally, instead of using the logical operation *and*, element wise products are used to approximate the non-differentiable intersection operation. To avoid a division by zero, +1 is added on the numerator and denominator.

Because many more pixels in the masks are 0 than 1, there is a class imbalance problem. It is a problem, because in this case a false positive gives a much higher loss than a false negative. For example, predicting only black would give an acceptable loss, while predicting only white pixels would not. Using the Dice coefficient as a loss function for training should make it invariant to this class imbalance problem as stated by Fausto Milletari et al. in [**?**].

The binary cross-entropy loss, also called Log loss, is defined by:

$$H_p(q) = -\frac{1}{N}\sum_{i=1}^{N} y_i \cdot log(p(y_i)) + (1-y_i) \cdot log(1-p(y_i))$$

For pixel values of 0 and 1, it adds $log(p(y))$ for each white pixel (y=1) and $log(1-p(y))$ for every black pixel (y=0) to the loss.

We quickly realised that the Dice-loss gives the best results for our problem and therefore used it to train the model. **To do** (??)

pytex$_fig('scripts/prepro_example.py', conf =' article/main.conf', caption =' Distributiondensitiesoft - statistics, showingtheregionswereVTAstructuralprojectionsexceedfunctionalactivationmoststrongly.vspace{-1em}', label =' dffn', options_pre =' centering', environment =' figure', figure_format =' pdf',)$

Data Set

The data set consists of 3D MR images taken from an aggregation of three studies; irsabi , opfvta [**?**], drlfom [**?**] and other unpublished data, acquired with similar parameters. **To do** (??)

The images are transformed into a standard space with one defined mask via SAMRI [**?**] and are thus defined in the same affine space. SAMRI is a data analysis package of the ETH/UZH Institute for Biomedical Engineering. It is equipped with an optimized registration workflow and standard geometric space for small animal brain imaging [**?**].

Because of variance in mouse brain anatomy and in the experiment setup, some of the transformed data do not overlap perfectly with the reference template. To filter these images out, most of the incongruent slices were removed manually from the data set.

For the registration of the images, a padding was needed to make the originally not affine space affine. Due to this, the 3D volumes present many zero-valued slices, some of them overlapping with the mask.**To do** (??) **??** Since it is not wanted for the model to predict a mask on black slices, the mask is set to zero where the image is as well. Because some pixels representing the brain tissue are zero-valued, holes result from this operation. To patch these, the function binary_fill_holes from scipy.ndimage.morphology [**?**] is used.

In the coronal view, each slice of the transformed data is originally of shape (63, 48), matching the reference space resolution of 200 µm. It is then reshaped into (64, 64) by adding a zero padding to the border.

Finally, the images are normalised by first clipping them from the minimum to the 99th percentile of the data in order to remove outliers and then divided by the maximum.

Data Augmentation

Because of diverse settings in the experiment setup, including animal manipulations causing artifacts, MR image quality can differ substantially between labs and even individual study populations. To account for these variations, we apply an extensive set of transformations to our data. This includes rotations of up to 90°, a width and height shift range of 30 pixels, a shear range of 5 pixels, zoom range of 0.2 and horizontal as well as vertical flips.

This not only increases the data set size but also makes it more representative of the general data distribution of Mice brain MR images and results in a model with a better generalisation capability.

Many more sophisticated methods have been tested, but it has been shown that one of the more successful data augmentation strategies is the simple transformations mentioned above [**?**].

Training

The model was trained slice wise, with the coronal view and 600 as the maximum number of epochs. The coronal view was chosen over the axial one, because the shapes of the masks are much simpler in the coronal view and thus easier to learn for the network. Additionally the coronal view has the advantage of higher resolution as the MR images were recorded coronally.

Because of the extensive transformations on the images (see section 2.3), the augmented data presents much variation. To alleviate the learning process of the model, we have first trained it on the data without augmentation and then on the augmented data. This has been shown to give better results: **To do** (??)

To improve the learning process of the network, two callbacks from Keras were used [?]. "ReduceLROnPlateau" reduces the learning rate when the validation loss has stopped improving and "EarlyStopping" stops the training when the validation loss has stopped improving for a number of epochs. The latter reduces computation time and prevents overfitting.

Evaluation

A major challenge of registration QC is that a perfect mapping from the measured image to the template is undefined. Similarity metrics are ill-suited for QC because they are used internally by registration functions, whose mode of operation is based on maximizing them. Extreme similarity score maximization is not a desired outcome, particularly if nonlinear transformations are employed, as this may result in image distortions which should be penalized in QC. Moreover, similarity metrics are not independent, so the issues arising from similarity score maximization cannot be circumvented by maximizing a subset of metrics and performing QC via the remainder. To address this challenge, we developed four alternative evaluation metrics: volume conservation, smoothness conservation, functional analysis, and variance analysis. In order to mitigate possible differences arising from template features, we use these metrics for multifactorial analyses — including both a template and a workflow factor.

Volume Conservation

??

Volume conservation is based on the assumption that the total volume of the scanned segment of the brain should remain roughly constant after preprocessing. Beyond just size differences between the acquired data and the target template, a volume increase may indicate that the brain was stretched to fill in template brain space not covered by the scan, while a volume decrease might indicate that non-brain voxels were introduced into the template brain space. For this analysis we compute a Volume Conservation Factor (VCF), whereby volume conservation is highest for a VCF equal to 1.

As seen in ??, we note that in the described dataset VCF is sensitive to the workflow (??), the template (??), but not the interaction thereof (??).

The performance of the Generic SAMRI workflow in conjunction with the Generic template is significantly different from that of the Legacy workflow in conjunction with the Legacy template, yielding a two-tailed p-value of ??. Moreover, the root mean squared error ratio strongly favours the Generic workflow ($\mathrm{RMSE}_{\mathrm{L}}/\mathrm{RMSE}_{\mathrm{G}} \simeq$??).

Descriptively, we observe that the Legacy level of the template variable introduces a notable volume loss (VCF of ??), while the Legacy level of the workflow variable introduces a volume gain (VCF of ??). Further, we note that there is a very strong variance increase in all conditions for the Legacy workflow (??-fold given the Legacy template, and ??-fold given the Generic template).

With respect to the data break-up by contrast (CBV versus BOLD, ??), we see no notable main effect for the contrast variable (VCF of ??). We do, however, report a notable effect for the contrast-template interaction, with the Legacy workflow and CBV contrast interaction level introducing a volume loss (VCF of ??).

Smoothness Conservation

A further aspect of preprocessing quality is the resulting image smoothness. Although controlled smoothing is a valuable preprocessing tool used to increase the signal-to-noise ratio (SNR), uncontrolled smoothness limits operator discretion in the trade-off between SNR and feature granularity. Uncontrolled smoothness can thus lead to undocumented and implicit loss of spatial resolution and is therefore associated with inferior anatomical alignment [?]. We employ a Smoothness Conservation Factor (SCF), expressing the ratio between the smoothness of the preprocessed images and the smoothness of the original images.

With respect to the data shown in ??, we note that SCF is sensitive to the template (??), the workflow (??), and the interaction of the factors (??).

The performance of the Generic SAMRI workflow in conjunction with the Generic template is significantly different from that of the Legacy workflow in conjunction with the Legacy template, yielding a two-tailed p-value of ??. In this comparison, the root mean squared error ratio favours the Generic workflow ($\mathrm{RMSE}_{\mathrm{L}}/\mathrm{RMSE}_{\mathrm{G}} \simeq$??).

Descriptively, we observe that the Legacy level of the template variable introduces a smoothness reduction (SCF of ??), while the Legacy level of the workflow variable introduces a smoothness gain (SCF of ??). Further, we note that there is a strong variance increase for the Legacy workflow (??-fold given the Legacy template and ??-fold given the Generic template).

Given the break-up by contrast shown in ??, we see only very weak effect sizes for the contrast variable (SCF of ??) and the contrast-template interaction (SCF of ??).

Functional Analysis

Functional analysis is a frequently used avenue for preprocessing QC. Its viability derives from the fact that the metric being maximized in the registration process is not the same output metric as that used for QC. The method is however primarily suited to examine workflow effects in light of higher-level applications, and less suited for wide-spread QC (as it is computationally intensive and only applicable to stimulus-evoked functional data). Additionally, functional analysis significance is documented to be sensitive to data smoothness [?], and thus an increased score on account of uncontrolled smoothing can be expected. For this analysis we compute the Mean Significance (MS), expressing the significance detected across all voxels of a scan.

As seen in ??, MS is sensitive to the workflow (??), but not to the template (??), nor the interaction of both factors (??).

The performance of the SAMRI Generic workflow (with the Generic template) differs significantly from that of the Legacy workflow (with the Legacy template) in terms of MS, yielding a two-tailed p-value of ??.

Descriptively, we observe that the Legacy level of the workflow variable introduces a notable significance increase (MS of ??), while the Legacy level of the template variable (MS of ??), and the interaction of the Legacy template and Legacy workflow (MS of ??) introduce no significance change. Furthermore, we again note a variance increase in all conditions for the Legacy workflow (??-fold given the Legacy template, and ??-fold given the Generic template).

With respect to the data break-up by contrast (??), we see no notable main effect for the contrast variable (MS of ??) and no notable effect for the contrast-template interaction (MS of ??).

Functional analysis effects can further be inspected by visualizing the statistic maps. Second-level t-statistic maps depicting the CBV and BOLD omnibus contrasts (common to all subjects and sessions) provide a succinct overview capturing both amplitude and directionality of the signal (??). Crucial to the examination of registration quality and its effects on functional read-outs is the differential coverage. We note that the Legacy workflow induces coverage overflow, extending to the cerebellum (????????), as well as to more rostral areas when used in conjunction with the Legacy template (????). Separately from the Legacy workflow, the Legacy template causes acquisition slice misalignment (????????). Positive activation of the Raphe system, most clearly disambiguated from the surrounding tissue in the BOLD contrast, is notably displaced very far caudally by the joint effects of the Legacy workflow and the Legacy template (??). We note that processing with the Generic template and workflow (????), does not show issues with statistic coverage alignment and overflow.

??

Variance Analysis

??

An additional way to assess preprocessing quality focuses on the robustness to variability across repeated measurements, and whether this is attained without overfitting (i.e. compromising physiologically meaningful variability). The core assumption of this analysis of variance is that adult mouse brains in the absence of intervention retain size, shape, and implant position throughout the 8 week study period. Consequently, when examining similarity scores of preprocessed scans with respect to the target template, more variation should be found across levels of the subject variable rather than session variable. This comparison can be performed using a type 3 ANOVA, modelling both the subject and the session variables. For this assessment we select three metrics with maximal sensitivity to different features: Neighborhood Cross Correlation (CC, sensitive to localized correlation), Global Correlation (GC, sensitive to whole-image correlation), and Mutual Information (MI, sensitive to whole-image information similarity).

?? renders the similarity metric scores for both the SAMRI Generic and Legacy workflows (considering only the matching workflow-template combinations). The Legacy workflow produces results which show a higher F-statistic for the session than for the subject variable: CC (subject: ??, session: ??), GC (subject: ??, session: ??), and MI (subject: ??, session: ??).

The Generic SAMRI workflow shows a reversing trend. Resulting data F-statistics are consistently higher for the subject variable than for the session variable: CC (subject: ??, session: ??), GC (subject: ??, session: ??), and MI (subject: ??, session: ??).

Discussion

The workflow and template design presented herein offer significant advantages in terms of reducing coverage overestimation, uncontrolled smoothness, and guaranteeing session-to-session consistency. This is most clearly highlighted by Volume Conservation (??), Smoothness Conservation (??), and Variance Analysis (??), where the combined usage of the SAMRI Generic workflow and template outperforms all other combinations of the multi-factorial analysis. Increased region assignment validity is also revealed in a qualitative examination of higher-level functional maps (??), where only the combination of the Generic workflow and template provides accurate coverage of the sampled volume for both BOLD and CBV fMRI data. iThese benefits are robust to the functional contrast (??????), with the Generic workflow-template combination being less or equally susceptible to the contrast variable, when compared to the Legacy workflow-template combination. The performance of the Generic workflow is more consistent across all metrics, as demonstrated by notable reductions of the standard deviation for both VCS, SCF, as well as MS (??????).

Closer model inspection reveals that in addition to the processing factor, the template factor is also a strong source of variability. The Legacy template induces both a volume and a smoothness decrease beyond the original data values (????). This clearly indicates a whole-volume effect, whereby a target template smaller than the recoded brain size causes a contraction of the brain during registration, resulting both in a volume and a smoothness loss. This effect can also be observed qualitatively in ??. We thus highlight the importance of an appropriate template choice, and strongly recommend usage of the Generic template on account of its better scale similarity to data acquired in adult mice.

The volume conservation, smoothness conservation, and session-to-session consistency of the SAMRI Generic workflow and template combination are further augmented by numerous design benefits (????). These include increased transparency and parameterization of the workflow (which can more easily be inspected and further improved or customized), veracity of resulting data headers, and spatial coordinates more meaningful for surgery and histology.

Quality Control

A major contribution of this work is the implementation of multiple metrics providing simple, powerful and robust QC for registration performance (VCF, SCF, MS, and Variance Analysis) and the release of a dataset [?] suitable for such multifaceted benchmarking — including the analysis of session-wise and subject-wise variability.

The VCF and SCF provide good quantitative estimates of distortion prevalence. The analysis comparing subject-wise and session-wise variance is an elegant avenue allowing the operator to ascertain how much a registration workflow is potentially overfitting, by differentiating between meaningful (inter-subject) and confounding (inter-session) variability. These metrics are relevant to both preclinical and clinical MRI workflow improvements, and could themselves be further optimized.

Global statistical power is not a reliable metric for registration optimization. Regrettably, however, it may be the most prevalently used if results are only inspected at a higher level — and could bias analysis. This is exemplified by the positive main effect of the Legacy workflow seen in ??. In this particular case, optimizing for statistical power alone would give a misleading indication, as becomes evident when all other metrics are inspected.

We suggest that a VCF, SCF and Variance based comparison, coupled with visual inspection of a small number of omnibus statistic maps is a feasible and sufficient tool for benchmarking workflows. We recommend reuse of the presented data for workflow benchmarking, as they include (a) multiple sources of variation (contrast, session, subjects), (b) functional activity with broad coverage but spatially distinct features, and (c) significant distortions due to implant properties — which are appropriate for testing workflow robustness. In addition to the workflow code [?], we openly release the re-executable source code [?] for all statistics and figures in this document. It is thus not just the novel method, but also the benchmarking process which is fully transparent and reusable with further data.

Conclusion

We present a novel registration workflow, entitled SAMRI Generic, which offers several advantages compared to the ad hoc approaches commonly used for small animal MRI. In depth multivariate comparison with a thoroughly documented Legacy pipeline revealed superior performance of the SAMRI Generic workflow in terms of volume and smoothness conservation, as well as variance structure across subjects and sessions. The metrics introduced for registration QC are not restricted to the processing of small animal fMRI data, but can be readily expanded to other brain imaging applications. The optimized registration parameters of the SAMRI Generic Workflow are easily accessible in the source code and transferable to any other workflows making use of the ANTs package. The open source software choices in both the workflow and this article's source code empower users to better verify, understand, remix, and reuse our work. Overall, we believe that using the SAMRI Generic workflow should facilitate and harmonize processing of mouse brain imaging data across studies and centers.

Methods

The slice-wise predictions of the model are reconstructed to a 3D mask via the command *Nifit1Image* from the neuro-imaging python package nibabel [?]. This is done using the same affine space as the input image.

For the training of the classifier, the data are separated into a Training, Validation and Test set with the help of the function *train_test_split* from the package sklearn.model_selection [?].

Supplementary Materials

??

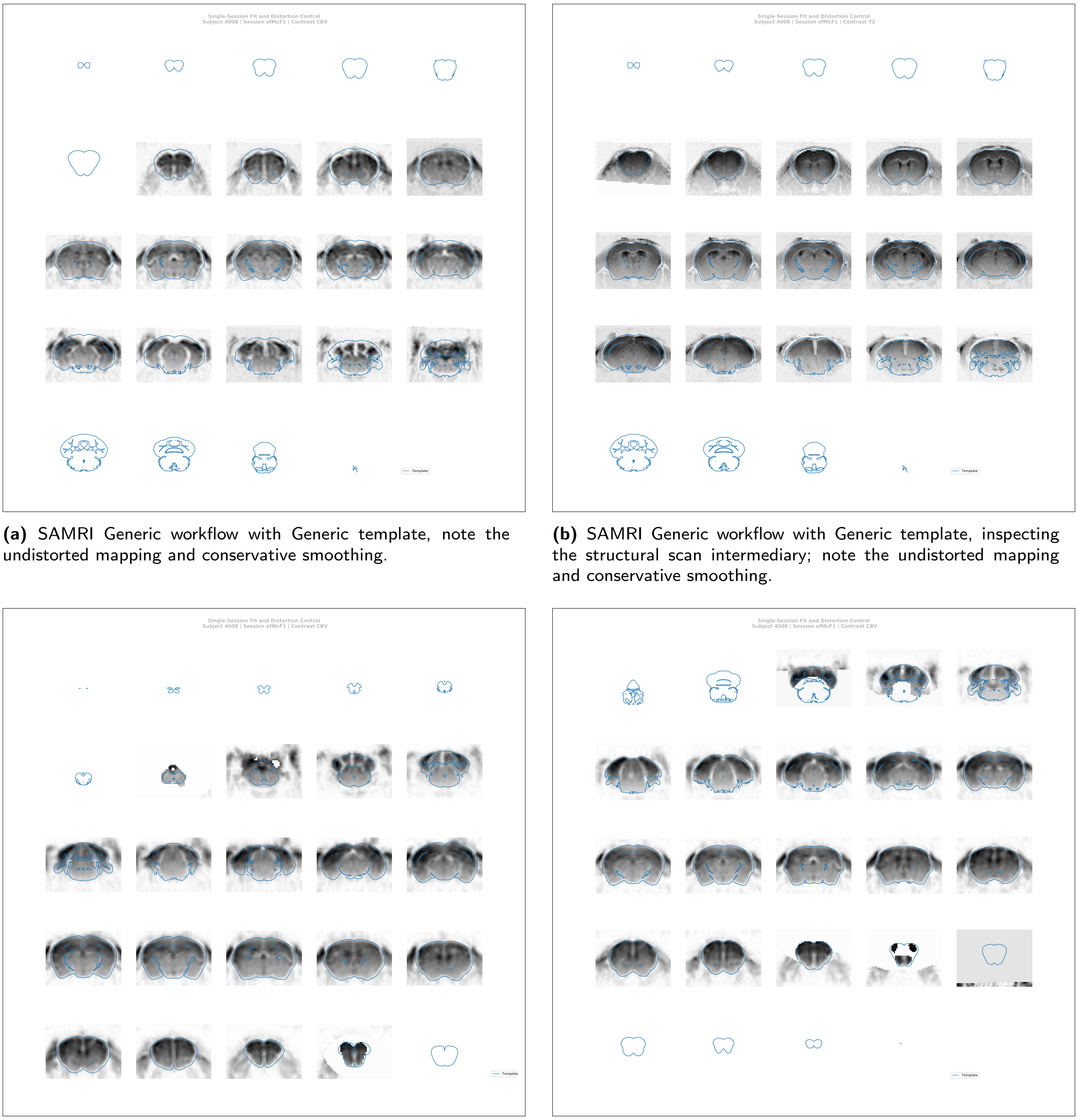
Single-Session Fit and Distortion Control
Subject 4008 | Session ofMcF1 | Contrast CBV
Template
Single-Session Fit and Distortion Control
Subject 4008 | Session ofMcF1 | Contrast T2
Template
Single-Session Fit and Distortion Control
Subject 4008 | Session ofMcF1 | Contrast CBV
Template
Single-Session Fit and Distortion Control
Subject 4008 | Session ofMcF1 | Contrast CBV
Template

(a) SAMRI Generic workflow with Generic template, note the undistorted mapping and conservative smoothing.

(b) SAMRI Generic workflow with Generic template, inspecting the structural scan intermediary; note the undistorted mapping and conservative smoothing.

(c) SAMRI Legacy workflow with Legacy template, note the strong smoothing and the mapping distortion in the rostral and caudal areas.

(d) SAMRI Legacy workflow with Generic template, note the strong smoothing and the mapping distortion in the rostral and caudal areas.

Figure S1: The SAMRI Generic workflow induces less smoothness, and provides more accurate coverage. Depicted are automatically created operator overview graphics, which allow a slice-by-slice (spacing analogous to acquisition) inspection of the registration fit. This representation affords a particularly detailed view of the preprocessed MRI data, and highly accurate template contours.

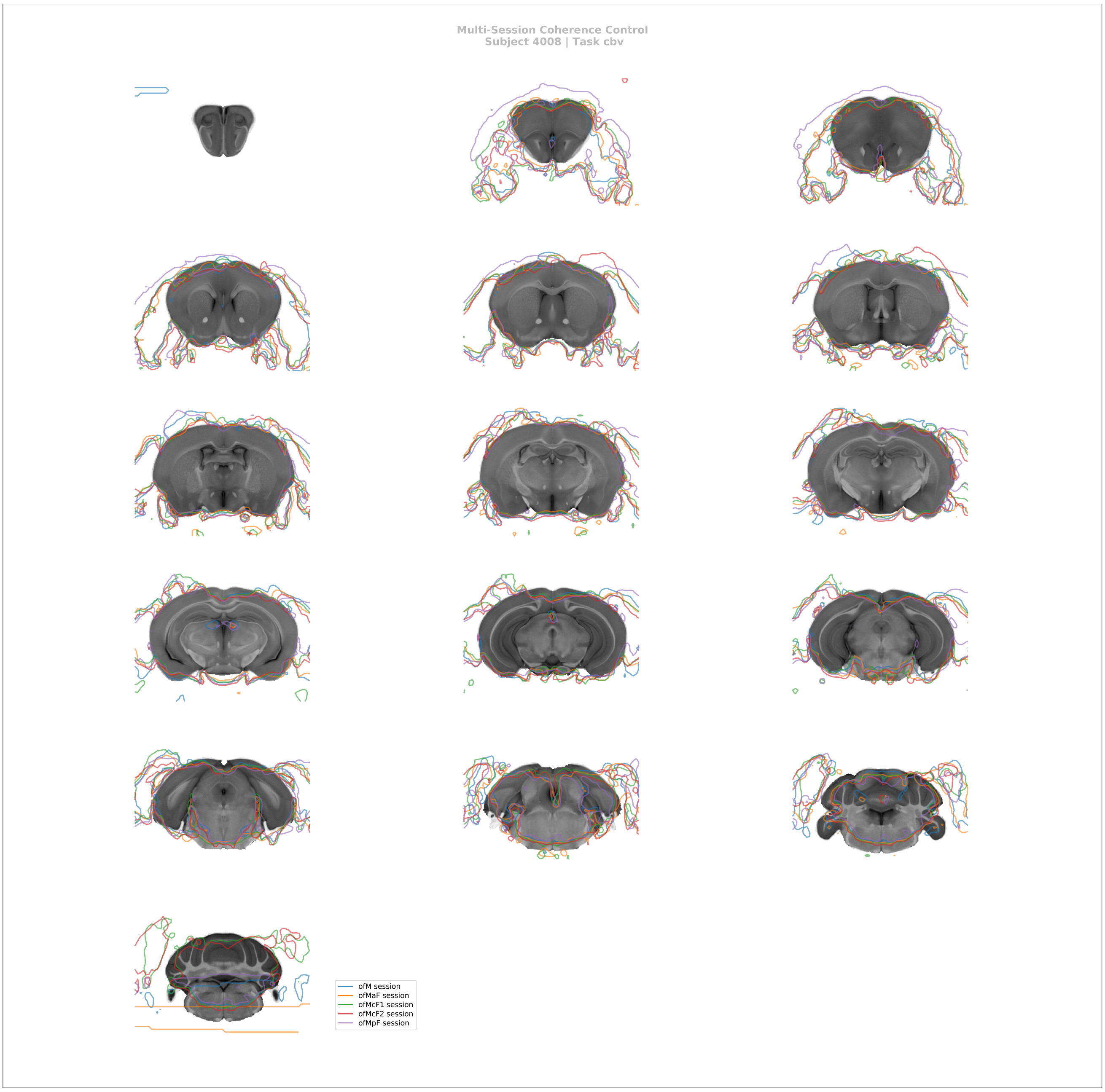

Figure S2: The SAMRI Generic workflow consistently maps high-salience features such as the implant site across sessions. Automatically created operator overview graphic, allowing a slice-by-slice (spacing analogous to acquisition) inspection of registration coherence. This representation permits a coarse assessment of registration consistency for multiple sessions — though at the cost of some clarity. Particularly, this visualization, allows an operator to track the position of high-amplitude fixed features across scans in order to ascertain coherence (similarly to what is automatically assessed by the Variance analysis of the session factor).

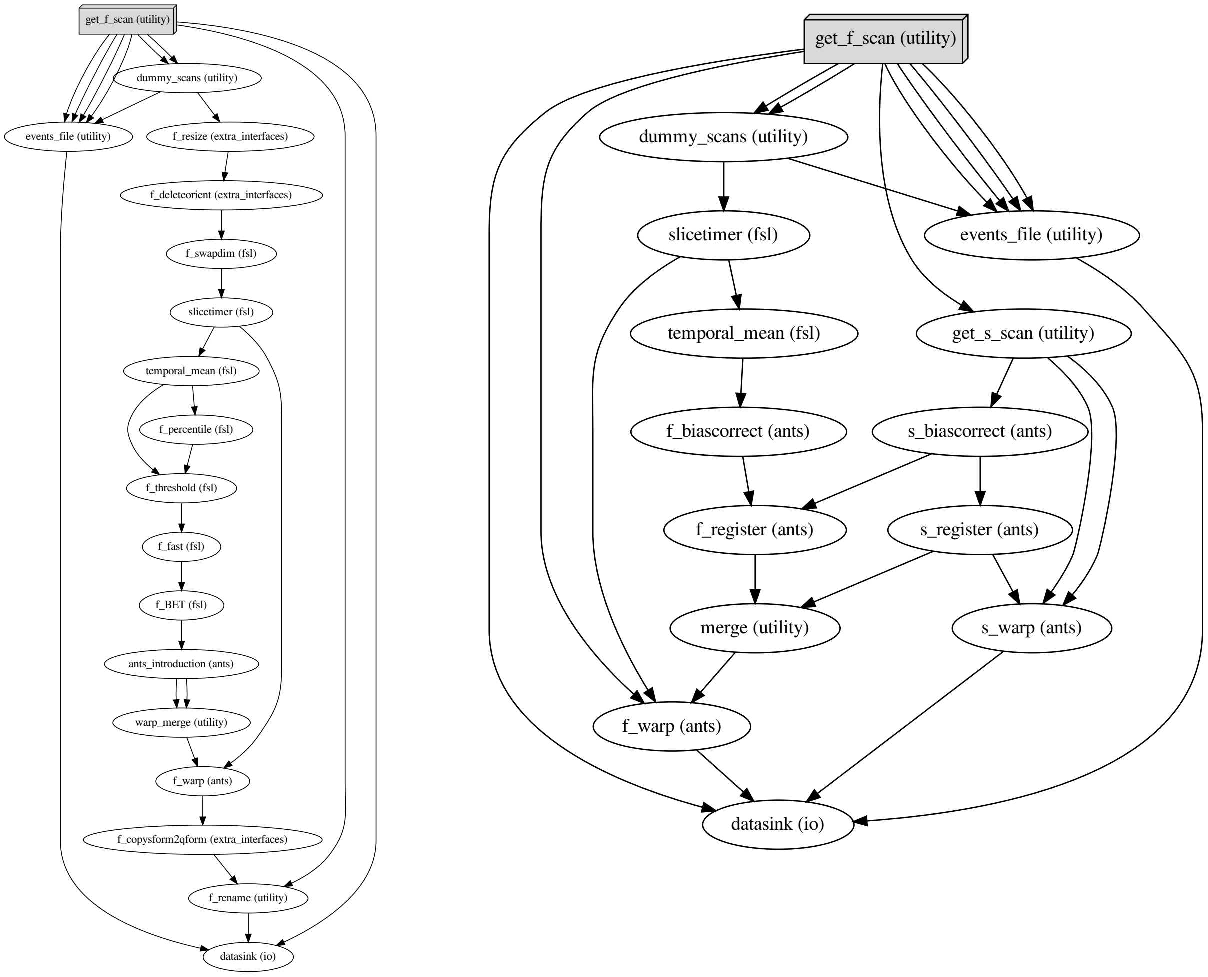

(a) "SAMRI Legacy" workflow, which is based on the `antsIntroduction.sh` function (and other functions with hard-coded parameters optimized for human brain registration), and also performs destructive affine manipulations.

(b) "SAMRI Generic" workflow, based on the `antsRegistration` function. The pipeline uses a higher-resolution structural scan intermediary for registration (note the two processing streams), which facilitates differential handling of anatomical variation and susceptibility artefacts. The function used is highly parameterized, and both of its instances — "s_register" and "f_register" — are supplied in the workflow with defaults optimized for mouse brain registration.

Figure S3: Directed acyclic graphs detailing the precise node names (as seen in the SAMRI source code) for the two alternate MRI registration workflows. The package correspondence of each processing node is appended in parentheses to the node name. The "utility" indication corresponds to nodes based on Python functions specific to the workflow, distributed alongside it, and dynamically wrapped via Nipype. The "extra_interfaces" indication corresponds to nodes using explicitly defined Nipype-style interfaces, which are specific to the workflow and distributed alongside it.